19th Brazilian Congress of Thermal Sciences and Engineering
November 06th-10th, 2022, Bento Gonçalves - RS - Brazil

COMMERCIAL DRINKING-FOUNTAIN EXPERIMENT, BASED ON ABNT NBR 16236

Matheus Henrique Cavalheiro Garros [1]
matheus.garros@gmail.com

Robson Leal da Silva [2, 3]
rlealsilva@hotmail.com

[1] Energy Engineer, graduated at UFGD – Universidade Federal da Grande Dourados.
[2] UFGD – Universidade Federal da Grande Dourados, FAEN – Faculdade de Engenharia, Dourados-MS, Brasil, CEP: 79.804-970
[3] PEM – Programa de Pós-Graduação em Engenharia Mecânica, UEM – Universidade Estadual de Maringá, Maringá-PR, Brasil, CEP: 87.020-900

Abstract. *This paper analyzed a commercial drinking-fountain, based on ABNT NBR 16232 to validate its sheet information, using an experimental and computational approach. In the experiment, a small structure was constructed, and two thermocouples measured the reservoir and water feeding temperatures. An Arduino sensor measured the temperature in the outlet of the expansion device and in the compressor outlet, to collect data for the simulation. The computational simulation used natural refrigerants such as R290, R600a, R744, and R717 as substitutes for R134a. The open-source software DWSIM executed the simulations. The conclusion was a disagreement between the sheet information and the experimental results: The information in the sheet (6 L/h) was not obtained in a test similar to the one proposed by the standard. The computational approach confirms that R290 and R600a are candidates for the drop-in of R134a, without compromising the COP or the system design (pressures and temperatures). A combination of experimental and simulation data showed the poor design of the heat-transfer evaporator-reservoir, with a very low heat transfer effectiveness (0,04).*

Keywords: *GWP, HFC, Hydrocarbons, drinking-fountain, energy.*

1. INTRODUCTION

Over the past years, a significant effort has been made to improve energy efficiency in several areas. ABNT standards have a key role in this subject with standards like NBR ISO 50.001 (ABNT, 2018) regarding efficient energy management systems. The ideas behind it are very suitable to areas as the refrigeration sector.

Small refrigeration devices are usually oversight towards their energy efficiency, even being common in several public establishments. Though most of those devices declare the energy consumption per unit of cold water produced, hardly ever a note informing the tests respected the current standard are found (NBR 16236, ABNT, 2013).

Along with that, several systems still use HFC as a working fluid, but Montreal (1987) and Kyoto Protocols (1997) have already set the deadline for high ODP (Ozone Depletion Potential) and GWP (Global Warming Potential) refrigerants. The current legislation situation in Brazil is show in Table 1.

Table 1. Current refrigerant situation in Brazil

Refrigerant	Import	Remark[(1)]
CFCs	Prohibited	In agreement with "Conama Settlement nº 267, 14/09/2000"
HCFCs	Restrict	Allowed to companies that have import quota, with Ibama approval, in agreement with Ibama Normative Ruling nº 4, 14/02/2018", expected a 100% reduction until 2040 (current 51.6%)
HFCs	Allowed	Allowed to companies that follow the current environmental legislation, with Ibama approval, expected an 80% reduction until 2045 (Kigali Amendment, 2016)

(1) Ibama (2021)

There are already alternatives in the market, such as R-290 (propane) and R600a (isobutane), which are ideal for commercial and residential applications. For a low charge of refrigerant, the hydrocarbons flammability is harmless. R-717 (ammonia) is dangerous for indoor applications but is still suitable for water-chiller applications.

Both hydrocarbons and ammonia are natural refrigerants and have an energy efficiency similar to the HFCs widely used. The opposite for R-744 (carbon dioxide), another natural refrigerant solution. Its low critical temperature (31,1°C) lowers the theoretical cycle efficiency in most applications. Still, it reaches the traditional cycle efficiency in mild climates, where the system doesn't operate under a transcritical cycle (Goetzler et al., 2014).

Recent studies have already shown the possibility of the replacement of R-134a using hydrocarbons. In vapor compression cycles (VCR), R-290 is more efficient than R-134a in several applications, considering both COP and exergy efficiency, and uses a lower refrigerant charge (Paula et al., 2020; Sánchez et al., 2017). R-600a and R-717 achieved similar results (Soni et al., 2022), where R-600a pointed out in terms of COP, and R717 in the mass-flow rate.

1.1 Objective

Analyze a small drinking-fountain (Manufacturer: Libell; Model: Press Baby), based on NBR 16236 (ABNT, 2013), to compare the experimental results with the information given by the manufacturer. Then, to model the system and simulate the cycle using other refrigerants, to compare the performance using low GWP working fluids.

2. METHODOLOGY

Two methodologies were employed: an experimental approach to analyze how the equipment performs under the standard scope and to set the boundary conditions for the simulations. Those provide the possibility to analyze the performance of the system using other refrigerants. The main characteristic of each simulated refrigerant is shown in Table 2.

Table 2. Refrigerant characteristics

Refrigerant	Flammability	Toxicity	GWP[(1)]
R134a	None	Low	1300
Carbon dioxide (R744)	None	Low	1
Ammonia (R717)	Low	High	0
Isobutane (R600a)	High	Low	3
Propane (R290)	High	Low	3

(1)Goetzler et al. (2014)

2.1 Experimental approach

To study the equipment profile based on the NBR 16236, a structure has been constructed, as shown in Figure 1. This is the base for a future climatic chamber, aiming for a better experimental approach, as advised by the reference standard (humidity and temperature control).

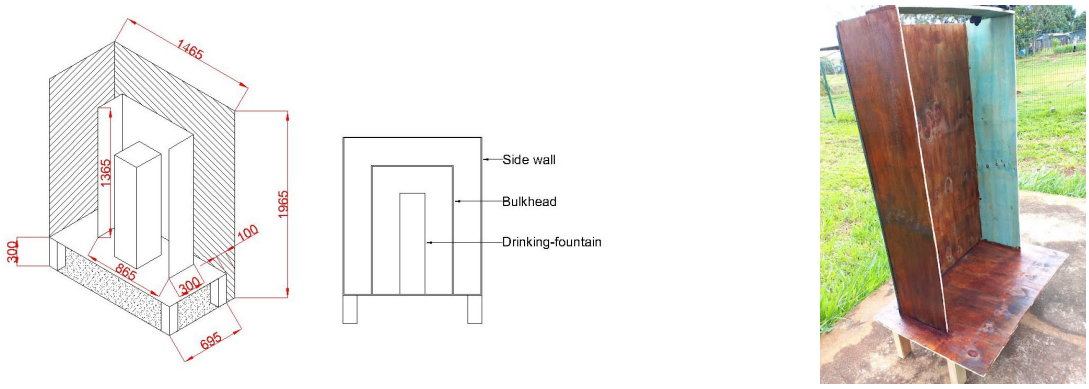

(a) Complete structure dimensions (b) Internal structure built

Figure 1. Test platform built based on NBR 16363 (ABNT, 1993)

Two thermocouples measured the water temperature at the device's inlet and inside the reservoir, and a mercury-in-glass thermometer measured the surrounding temperature. The water outlet volume was measured using a 2 L Erlenmeyer flask. The reservoir and surrounding temperatures were checked every 15 minutes, annotating the inlet temperature at the beginning and end of the water removal.

The removal started when the water achieved the set temperature – the lowest configurable temperature - and occurred until the reservoir was between 12°C and 13°C, a little more than the established standard (10°C, with a 0,5°C tolerance) but still acceptable to the analysis. The hole process repeated 5 times. Figure 2 illustrates the experimental setup.

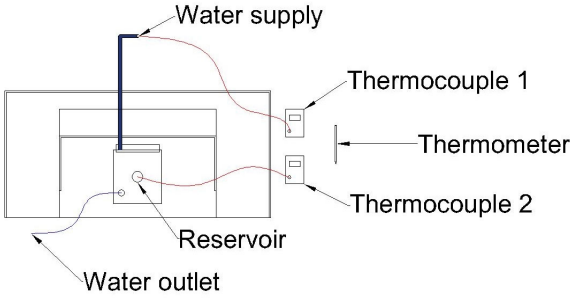

Figure 2. Schematic of the data-measuring process

Table 3 displays the instrumentation data. The methodology presented in Albertazzi et al. (2018) and Neto (2012) served as a reference to calculate the instruments' uncertainties. The final result is highly dependent on the calibrator's uncertainty.

Table 3. Instrumentation data

Instruments[(1)]	**Measurement Uncertainty (°C)**	**Maximum correction (0°C to 15°C)**
1 - THR-1300	2.3	-0.5
2 - THR-150	2.2	1.3
Thermometer	0.5	0.0
Arduino MAX 6675	2.2	1.6
2 L Erlenmeyer	0.2	0.0

[(1)]Thermocouples calibrated using PC-321 (Instrutherm)

Along with all the measurements, the voltage and current of the compressor are taken at different time steps, in order to calculate the mean voltage and current, to estimate the compressor required power.

$$\dot{W}_c = Vi \tag{1}$$

Using the removed volume of each step (expect the first one, as defined by the standard), V_r is defined as the mean removed volume. C_f is the mean time the reservoir needed to achieve the set temperature. The refrigeration capacity, in L/h, is established in Eq. 2.

$$C_r = \frac{V_r}{C_f} \tag{2}$$

Since the compressor works on an on/off cycle, it operates on a constant power until the setpoint is reached. So, it is possible to define the energy used for every volume unit of cooled water (Eq. 3).

$$C_e = \frac{P_e}{C_r} \tag{3}$$

The mean heat transfer between the evaporator and the reservoir (Eq. 4) is estimated using the mass of water in the reservoir (mw), the specific heat of water (cp), and initial and final temperatures (Ti and Tf), and meantime of the removal.

The specific heat of liquid water, in the range of 0°C to 25°C is almost constant (4.22 and 4.18 kJ/kg.K, respectively, Tab. A3, Çengel and Boles, 2013), therefore, assuming a mean value of 4.20 kJ/kg.K for the calculations should not imply on relevant errors.

The technical sheet of the equipment informs a 3,6L of water capacity in the reservoir. The water density at 0°C is 1000 kg/m³, and at 25°C is 997 kg/m³ (Tab. A3, Çengel and Boles, 2013), a mean value of 998.5 kg/m³, resulting in a total of 3.5946 kg of water in the reservoir.

$$\dot{Q}_w = \frac{m_w c_p (T_i - T_f)}{\Delta t} \tag{4}$$

2.2 Computational approach

The open-source software DWSIM (Mariani et al., 2019; Mastellone et al., 2020) executed the simulations, using the Peng-Robinson property package to estimate the mixtures' properties. The water-fountain refrigeration cycle is the well-known four-stage cycle, where the capillary tube was modeled as a throttling valve. Figure 3 represents the system.

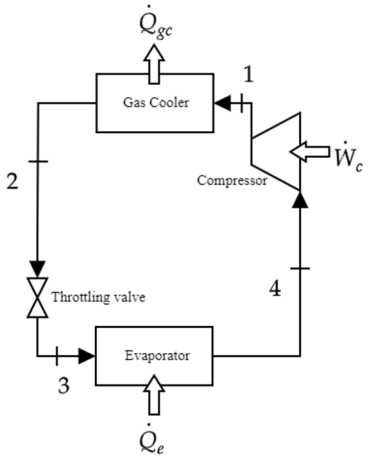

Figure 3. Four-stage refrigeration cycle

Thermocouples in states 2 and 3 estimated the set temperatures (MAX 6675, controlled via Arduino), decoupling the systems' thermostat. Figure 4 shows the results used to set saturation pressures. Refrigeration cycles operate using sub-cooling (condenser) and super-heating (evaporator), so the model considered a 5°C degree. The first thermocouple measured near 35°C in stage 2, setting the condensation pressure as the one for 40°C. In stage 3, the second thermocouple measured a near 0°C (the reference for the saturation pressure), setting a 5°C temperature the inlet temperature in the compressor.

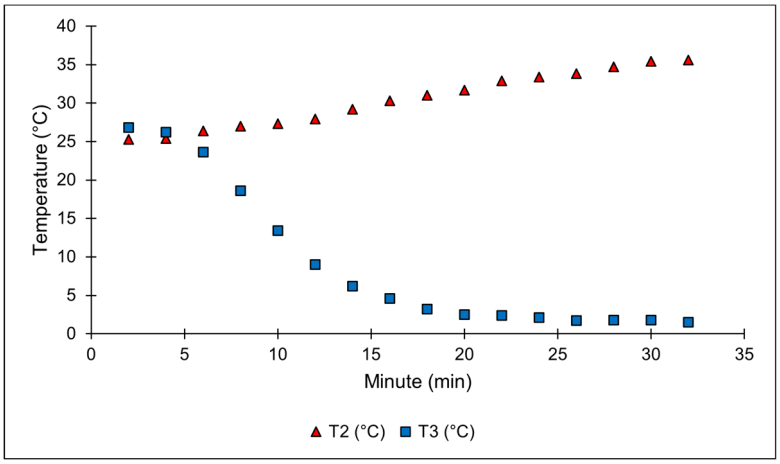

Figure 4. Temperature measurements to define the boundary conditions

The compressor efficiency is highly dependent on the pressure ratio, so the same is calculated via an expression (Eq. 5) suggested by Brown et al. (2002), where θ refers to the pressure ratio (P_1/P_4).

$$\eta_c = 0.9343 - 0.4478\theta \tag{5}$$

And last, the correct mass-flow rate depends on the power required by the compressor (Eq. 6), which is experimentally measured, using the voltage and current.

$$\dot{W}_c = \dot{m}(h_1 - h_4) \tag{6}$$

The conditions to model the R134a cycle are exposed in Table 4.

Table 4. Boundary conditions for the simulation using R134a

State/variable	**Condition**
P_1	Saturation pressure for 40°C
2	35°C ($P_1 = P_2$)
P_3	Saturation pressure for 0°C
4	5°C ($P_3 = P_4$)
$\dot{m}$	Based on $\dot{W}_c$ (measured experimentally), 0.13 kW
η_c	Based on Brown et al. (2002)

The simulation data allows an estimative for the heat transfer effectiveness (Eq. 7), since the maximum heat transfer is the refrigeration capacity of the simulation, and the actual heat transfer between evaporator and reservoir are known data.

$$\varepsilon = \frac{\dot{Q}_w}{\dot{Q}_e} \tag{7}$$

The results of the R134a simulations allow simulating the cycle using other refrigerants as working fluids, such as R290 (propane), R600a (isobutane), R744 (carbon dioxide), and R717 (ammonia), being all of them natural refrigerants, with very low GWP and zero ODP.

The refrigeration capacity (Eq. 8) of R134a is the contour condition instead of the power required by the compressor, so the output of all the cycles would be the same (time to refrigerate). The refrigeration capacity used in all simulations with the natural refrigerants was 0.62 kW.

$$\dot{Q}_e = \dot{m}(h_4 - h_3) \tag{8}$$

With all the results, the main analysis is based on the COP (Eq. 9),

$$COP = \frac{\dot{Q}_e}{\dot{W}_c} \tag{9}$$

Compressor outlet pressure, temperature, efficiency (P_1, T_1 and n_c), and mass-flow rate.

3. RESULTS AND DISCUSSION

3.1 Experimental Results

Figure 5 shows the temperature (a) and time (b) during the experiment. It is noticeable that the maximum and minimum temperatures were almost constant during the experiment, respecting the limits imposed in the methodology (water removal stops between 12°C and 13°C and starts at the turning-off of the compressor). The time between each removal tends to decrease with the progress of the experiment but achieves a limit of 1.75 h after the three first water removals.

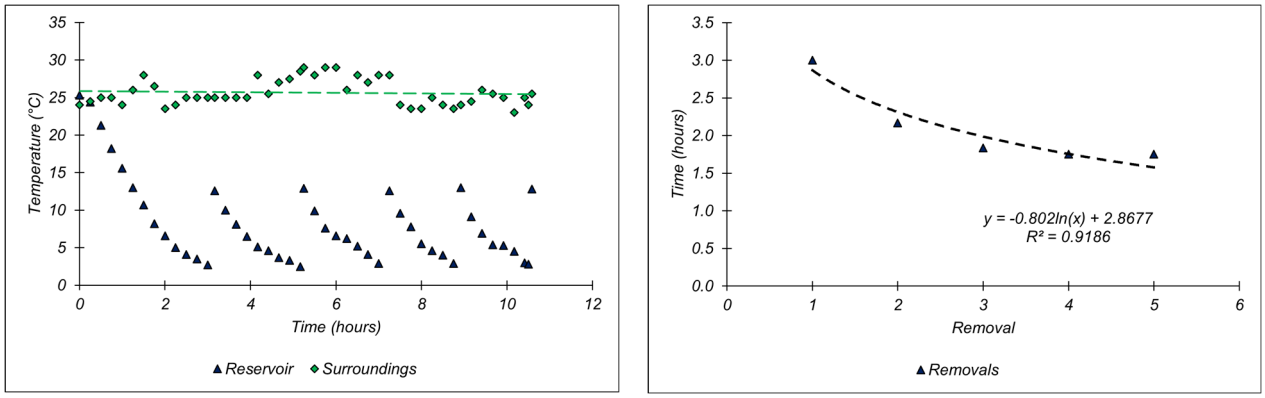

(a) Temperatures over the experiment time (b) Time between the removals

Figure 5. Experiment details: Temperature and time

Table 5 summarizes the main data collected during the experiment. The first removal is discarded as recommended, and the next 4 removals are used in the calculations. As expected, all the final temperatures during the removal were between the interval of 12°C to 13°C.

Table 5. Experimental data

Removal	Time (h)	Total time (h)	Water removed (L)	Minimal feeding temp. (°C)	Maximum feeding temp. (°C)	Start temp. (°C)	End temp. (°C)
1	3.00	3.00	1.6	27.5	29.6	2.7	12.6
2	2.17	5.17	1.3	26.5	28.7	2.5	12.9
3	1.83	7.00	1.3	26.0	27.9	2.9	12.6
4	1.75	8.75	1.7	28.0	28.	2.9	13.0
5	1.75	10.50	1.6	23.2	24.0	2.8	12.8

Table 6 shows the data after all the calculations. The general expression used to calculate the uncertainty of each measurement was the square root of the sum of the standard uncertainty and the measurement uncertainty (relative to the instrument used). For the indirect measurements an uncertainty propagation approach was used (Albertazzi et al, 2018).

Table 6. Final data

Magnitude	Value	Uncertainty
$T_{surroundigs}$ (ºC)	25.9	1.9
$T_{feeding}$ (ºC)	26.6	3.1
T_{start} (ºC)	2.8	2.2
T_{end} (ºC)	12.8	2.2
V_r (L)	1.5	0.3
C_f (h)	1.9	0.2
C_r (L/h)	0.8	0.2
V_{mean} (V)	126.0	0.9
I_{mean} (A)	1.0	0.1
P_{mean} (kW)	0.13	0.01
C_e (kWh/L)	0.17	0.06

The calculated data and the manufacturer sheet comparison make an inconsistency appears. The "refrigeration capacity" referred to as 6.0 L/h is absolutely different from the calculated (C_r) 0.8 L/h. Even though the surroundings were not always at 25°C, as suggested for this measurement, the temperature hasn't varied much. In newer sheets from the same manufacturer (Libell Press Star – similar drinking fountain), the chilled water supply capacity (understood as the "refrigeration capacity") is between 1.5 to 1.3 L/h, still far from the tested values, and without any mention to the experimental proceedings used.

3.2 Computational Results

Table 7 displays the main results of the simulations. All simulations have the same refrigeration capacity, calculated for R-134a in the methodology (Eq. 8) and equal to 0.62 kW. The results obtained with the R-134a simulation are the reference for comparisons.

Table 7. Simulation results

Property	R134a	R290	R600a	R744	R717
T_1 (ºC)	53.40	53.95	46.36	89.67	128.83
W_c (kW)	0.13	0.13	0.13	0.23	0.14
COP	4.76	4.62	4.65	2.66	4.53
$\dot{m}$ (kg/s)	3.99E-03	2.15E-03	2.23E-03	4.80E-03	5.49E-04
P_1 (MPa)	0.95	1.38	0.53	8.99	1.55
θ	3.30	2.88	3.37	2.57	3.62
η	78.7%	80.5%	78.3%	81.9%	77.2%

Figure 7 shows several comparisons between data. Figure 7a shows the relative values of COP: R-290, R-600a, and R-717 have similar performance compared to R134a. The worst performance occurs when using R744. The transcritical cycle (Figure 6) has several efficiency losses: The gas cooling process (no condensation before the throttling), the rejection loss due to the higher CO2 temperature after compression, and the throttling process, which has a great entropy difference (Shan, 2020).

(a) (b)

Figure 6. Subcritical (a) and transcritical (b) carbon-dioxide refrigeration cycles

A surprising result comes from Figure 7b: the compressor efficiency is higher using R-744. It is inversely proportional to the compressor ratio, and the R-744 cycle has the lowest. R-290 is more efficient too, and R-600a is similar to R-134a.

The worst working fluid in this scenario is R-717, which has a higher compression ratio. It justifies the high compressor outlet temperature (Figure 7c). The transcritical R-744 cycle, with the lowest compression ratio, has the 2nd highest temperature.

Figure 7d confirms that the transcritical cycle operates at very high pressures. All the working fluids are in the 0 – 2 MPa range, and R744 is in the 8 – 10 MPa range.

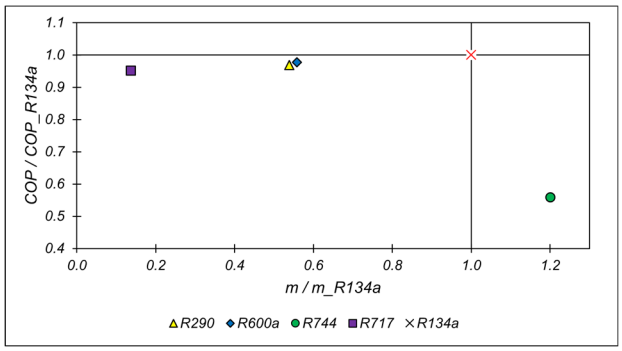

(a) Relative COP as a function of mass-flow rate

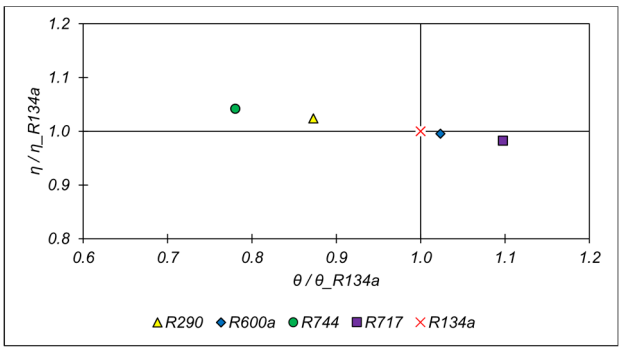

(b) Relative compressor isentropic efficiency as a function of compression ratio

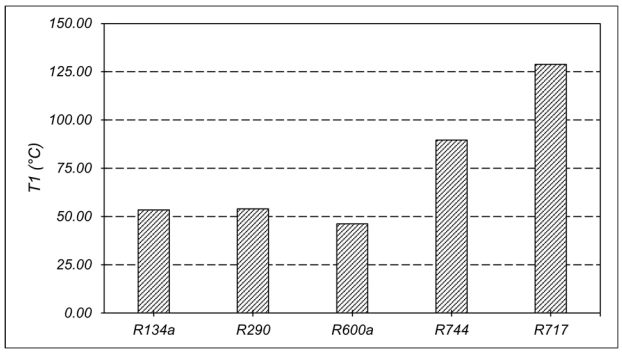

(c) Compressor outlet temperature

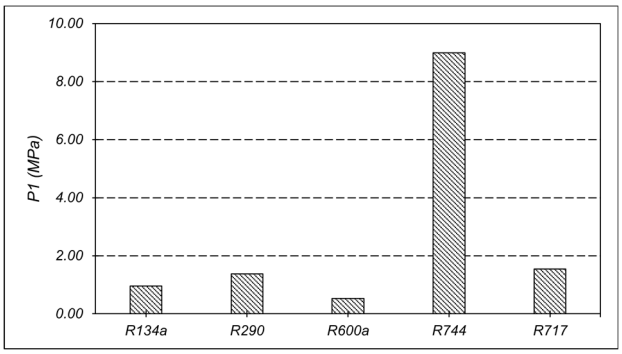

(d) Compressor outlet pressure

Figure 7. Simulations results

Both R290 and R600a are strong candidates to the *drop-in* of R134a, achieving similar characteristics and performance, being an eco-friendly working fluid.

3.3 Possible Heat Transfer Improvements

Using the data collected (Table 5), it's conclusive that the time of each removal tends to 1.75 h, equal to 6,300 s, so, using Eq. 4., a mean heat transfer of 0.024 kW is estimated. Knowing the mean power required by the compressor during the water-cooling process is 0.13 kW, the real COP of the couple evaporator + reservoir is 0.18, with a 0.04 heat transfer effectiveness (Eq. 7).

It's undeniable that the heat transfer between the evaporator and the water reservoir is the worst part of the equipment design and needs reviewing to improve energy efficiency.

4. CONCLUSION

This paper analyzed two situations: experimental (based on the reference standard) and computational (carried on DWSIM).

The experimental approach allowed us to notice the deficiencies of the drinking fountain to follow current standards, not having a reference for the values shown in the sheet, being very different from what was achieved (0.8 L/h in comparison with the 6.0 L/h indicated).

The computational approach showed the possibility to use R290 and R600a as substitutes for R134a in this sector. They have similar COP values, similar compression outlet temperatures, and operating pressures, combined with a very low GWP.

Combining the experimental and computational approaches, another great conclusion: The design of the heat-transfer evaporator – reservoir is poor and needs to be greatly improved.

Changing to an eco-friendly option like the natural refrigerants proposed, but with low energy efficiency, will not be a long-term solution, since the high energy consumption still contributes to the indirect increase of global warming.

5. REFERENCES

ABNT NBR 12863. *Refrigerators, freezers, cabinets and similar household appliances -Installation of appliances – Standardization*. ABNT, 1993, pp. 5.

ABNT NBR 16236. *Appliance for supplying drinking water with incorporated cooling — Performance requirements*. ABNT, 2013, pp. 8.

ABNT NBR ISO 50001. *Energy management systems — Requirements with guidance for use*. ABNT, 2018, pp. 34.

Albertazzi, A., Souza, A. R., *Fundamentals of Scientific and Industrial Metrology*. Manole Press, São Paulo, 2018, ISBN: 978-85-204-3375-1.

Çengel, Y.A. and Boles, M.A., 2013. *Thermodynamics*. Mc Graw Hill, Porto Alegre, 7th edition.

Goetzler, W., Shuterland, T., Rassi, M. and Burgos, J., 2014. "Research & development roadmap for next-generation low global warming potential refrigerants". US Department of Energy, Technical Report, https://doi.org/10.2172/1219983. Accessed 11 June 2021.

Ibama. "Montreal Protocol" In portuguese. <http://www.ibama.gov.br/emissoes/camada-de-ozonio/protocolo-de-montreal>.

Instrutherm LTDA. "Instructions Manual: Portable Digital Calibrator Model PC-321". <https://www.instrutherm.com.br/media/hexaattachment/products/attachments/p/c/pc-321_vers_pdf_1.pdf>.

Libell. "Equipment Technical Sheet – Libell Press Baby" In portuguese. < http://rfsites.com.br/libell/press-baby/ >.

Libell. "Equipment Techinal Sheet – Libell Press Star" In portuguese. < https://drive.google.com/file/d/19ZNRaZXV5via1TBTkFGIim49zV2WwgxB/view>.

Mariani, A., Mastellone, M.L., Marrone, B., Pratti, M.V. and Unich, A., 2019. "An organic Rankine cycle bottoming a diesel engine powered passenger car". *Energies*, Vol. 12, No. 2: 314, https://doi.org/10.3390/en13020314.

Mastellone, M.L., Mariani, A., Misso, E., Marrone, B., Unich, A. and Zaccariello, L., 2020. "Performance comparison of different thermal fluids in concentrating solar plants". *5th Thermal and Fluids Engineering Conference*. New Orleans, LA, USA.

Neto, João C. S., *Metrology and Dimensional Control*. Elsevier Press LTDA, Rio de Janeiro, 2012, ISBN 978 -85 -352 -5579-9.

de Paula, C. H., Duarte, W. M., Martins Rocha, T. T., de Oliveira, R. N., Torres Maia, A. A. "Optimal design and environmental, energy and exergy analysis of a vapor compression refrigeration system using R290, R1234yf, and R744 as alternatives to replace R134a". *International Journal of Refrigeration*, Vol. 113, 2020, pp. 10-20, ISSN 0140-7007, https://doi.org/10.1016/j.ijrefrig.2020.01.012.

Sánchez, D., Cabello, R., Llopis, R., Arauzo, I., Catalán-Gil, J., Torrella, E. "Energy performance evaluation of R1234yf, R1234ze(E), R600a, R290 and R152a as low-GWP R134a alternatives". *International Journal of Refrigeration*, Vol. 74, 2017, pp. 269-282, ISSN 0140-7007, https://doi.org/10.1016/j.ijrefrig.2016.09.020.

Shan, A.N.M N. U. "A Review of Trans-critical CO2 refrigeration cycle". *Proceedings of the International Conference on Industrial & Mechanical Engineering and Operations Management*, 2020, < http://www.ieomsociety.org/imeom/256.pdf>.

Soni, S., Mishra, P., Maheshwari, G., Verma, D. S. "Comparative energy analysis of R1234yf, R1234ze, R717 and R600a in Vapour Compression Refrigeration system as replacement of R134a". *Materials Today: Proceedings*, Vol. 56, Part 3, 2022, pp. 1600-1603, ISSN 2214-7853, https://doi.org/10.1016/j.matpr.2022.03.206.

6. RESPONSIBILITY NOTICE

The author(s) is (are) the only responsible for the printed material included in this paper.